Comprehensive analysis method for (d,p) stripping reactions

N. Keeley,* N. Alamanos, and V. Lapoux
CEA/DSM/DAPNIA/SPhN Saclay, 91191 Gif-sur-Yvette Cedex, France
(Received 22 March 2004; published 7 June 2004)

The (d,p) stripping reaction has proved a useful tool for probing single particle aspects of nuclear structure. With the advent of beams of exotic nuclei there has been renewed interest in charged particle spectroscopy and (d,p) stripping in particular as a means of investigating the structure of neutron-rich nuclei via reactions in inverse kinematics. The distorted wave Born approximation was shown to be inappropriate for the analysis of (d,p) reactions some 30 years ago, due to the importance of the deuteron breakup channel. While the simple adiabatic model has been demonstrated to work rather well in this context, modern computing facilities enable a more realistic treatment of the deuteron breakup process via the continuum discretized coupled channels procedure to be included in (d,p) calculations. In this work we present a comprehensive analysis method for (d,p) reactions using CDCC to model deuteron breakup and the Reid soft-core nucleon-nucleon potential to calculate the deuteron internal wave function. The model is tested against $^{12}C(d,p)$ data at incident deuteron energies of 15 and 30 MeV where all the necessary ancillary data are available. It is then applied to the $^{10}Be(d,p)$ reaction at 12 and 25 MeV where only the transfer cross section data are available.

DOI: 10.1103/PhysRevC.69.064604 PACS number(s): 25.45.Hi, 24.10.Eq

I. INTRODUCTION

The (d,p) stripping reaction has long been used as a means of probing the single particle structure of nuclei. In particular, through distorted wave Born approximation (DWBA) analyses it has been used to determine the orbital angular momentum and spectroscopic factors of specific states in the recoil nucleus. However, DWBA calculations are often unable to fit the data without the use of a lower radial cutoff or similar rather arbitrary devices. It was demonstrated some 30 years ago that deuteron breakup effects have an important influence on the (d,p) stripping reaction (see, e.g., Refs. [1–4]) that explains these *ad hoc* adjustments to the DWBA. The adiabatic model of Johnson and Soper [1,2], which includes deuteron breakup effects in an approximate way through a redefinition of the "deuteron" distorted wave, provides considerably improved agreement with (d,p) data for a wide range of targets and deuteron energies in the range 20–55 MeV compared with conventional DWBA, without the need for radial cutoffs or similar devices.

Although the adiabatic model has proved remarkably successful it does contain a number of simplifying assumptions, most notably the neglect of the deuteron excitation energy. More accurate treatments of deuteron breakup using the continuum discretized coupled channels (CDCC) approach have been developed, see, e.g., Refs. [4–7] and the review article of Austern *et al.* [8]. These calculations were able to provide very good descriptions of deuteron elastic scattering angular distributions, and showed that the adiabatic approximation compares very well with the more accurate calculations for the elastic channel. However, the CDCC method has also been used to model the effect of deuteron breakup within coupled channels Born approximation (CCBA) calculations for deuteron stripping [8,9], which showed that the adiabatic model description of the breakup contribution to stripping is systematically too small compared to the more accurate calculations.

Most of these calculations used a simplified $n-p$ potential of Gaussian form, an exception being those of Rawitscher and Mukherjee [5] which used the Reid soft-core potential [10], although Yahiro *et al.* [6] found that the use of a soft-core potential had little effect on the results for elastic scattering and breakup. Nevertheless, in the context of a comprehensive (d,p) stripping calculation the explicit inclusion of the D-state component of the deuteron ground state is desirable, as it has been found to have a significant effect on the (d,p) cross section when the orbital angular momentum of the transferred neutron is sufficiently large, $\ell=3$ [11]. The inclusion of the D-state is essential for the description of the tensor analyzing powers, T_{2q}, regardless of transferred ℓ value [12–15].

Previous calculations of (d,p) stripping using the CDCC method to model deuteron breakup have included other approximations (simplified $n-p$ potential, use of zero-range CCBA with finite-range correction). While these approximations are expected to work well in most circumstances, a truly comprehensive calculation that includes all effects on the same footing is desirable. Such a calculation is particularly timely with the current renewed interest in the use of (d,p) reactions as spectroscopic tools for radioactive nuclei by means of reactions in inverse kinematics.

In this work we present a method that brings together the various elements into a single comprehensive calculation that employs CDCC to model deuteron breakup, the full finite-range coupled reaction channels (CRC) method for the transfer component and the Reid soft-core nucleon-nucleon potential to calculate the $n-p$ wave functions. Two-step transfer paths proceeding via excited states of the target nucleus are also included in a natural way. The method is first applied to data for the $^{12}C(d,p)^{13}C$ reaction at incident deuteron energies of 15 and 30 MeV where appropriate d

*Electronic address: nkeeley@cea.fr

TABLE I. Optical model parameters for $p+^{12}$C, $n+^{12}$C and $p+^{13}$C obtained by fitting the data of Sydow *et al.* [26], McDaniel *et al.* [29], and Weller *et al.* [24] at incident nucleon energies of 7.5, 7.48, and 16.75 MeV, respectively. The real parts of the potentials are of volume Woods-Saxon form, while the imaginary parts are of Woods-Saxon derivative form.

	V	r_V	a_V	W_D	r_D	a_D	V_{SO}	r_{SO}	a_{SO}	r_C
$p+^{12}$C	52.91	1.138	0.6346	1.72	1.13	0.5462				1.13
$n+^{12}$C	97.0	1.4	0.37	15.0	1.19	0.4				
$p+^{13}$C	65.22	1.106	0.613	4.01	1.144	1.096	4.98	0.956	0.616	1.25

$+^{12}$C elastic and inelastic and $p+^{13}$C elastic scattering data are available. We then analyze transfer data for the ^{10}Be$(d,p)^{11}$Be reaction at incident deuteron energies of 12 and 25 MeV as an example of its application to data for a radioactive nucleus.

Section II describes the method in detail and its application to the ^{12}C$(d,p)^{13}$C data. The results for the ^{10}Be$(d,p)^{11}$Be reaction are presented in Sec. III. In Sec. IV we present our conclusions and indicate directions for future work.

II. CALCULATIONS FOR THE ^{12}C$(d,p)^{13}$C SYSTEM

As a test of the procedure it was first applied to data for the ^{12}C$(d,p)^{13}$C stripping reaction at incident deuteron energies of 15 [16,17] and 30 MeV [18]. Data are available for $d+^{12}$C elastic scattering at 15 [19] and 29.5 MeV [20] and for inelastic scattering to the 4.44 MeV ^{12}C 2^+ state at 15 [21] and 28 MeV [22,23]. Suitable $p+^{13}$C elastic scattering data for the exit channel are also available at incident proton energies of 16.75 [24] and 30.4 MeV [25]. Finally, as the deuteron breakup model requires neutron and proton plus target potentials at half the incident deuteron energy, it would be desirable to have the appropriate nucleon elastic scattering data. Such data are available for $p+^{12}$C at 7.5 [26], 7.55 MeV [27], 14.7 and 15.2 MeV [28] and for $n+^{12}$C at 7.48 [29] and 15 MeV [30]. Thus this system provides a severe test of the model, as all the inputs may be tested against appropriate data. All calculations described below were carried out using the code FRESCO, version FRXY.1h [31].

The calculations employed the CDCC method to model deuteron breakup and the post form of the CRC formalism for the neutron transfer component. The CDCC part of the calculations was similar to that described in Rawitscher and Mukherjee [5] and Yahiro *et al.* [6]. The $n-p$ wave functions were calculated using the Reid soft-core potential [10]. Following the work of Yahiro *et al.* [6] the $n-p$ relative orbital angular momentum was limited to $\ell=0,2$, it being found that contributions from $\ell=1,3$, and 4 were negligible. The $n-p$ continuum was discretized in $n-p$ relative momentum (k) space into bins of width $\Delta k=0.125$ fm^{-1}, again following Yahiro *et al.* [6]. The continuum was truncated at values of $k_{max}=0.5$ fm^{-1} and $k_{max}=0.625$ fm^{-1} for incident deuteron energies of 15 and 30 MeV, respectively. Yahiro *et al.* [6] found that a k_{max} of 1.5 fm^{-1} was necessary for convergence for the $d+^{58}$Ni system at an incident deuteron energy of 80 MeV. However, we found that the smaller values were adequate for the present case. Through the use of the Reid potential the model includes couplings between different $n-p$ relative angular momentum values as well as the continuum-continuum couplings between different bins.

The deuteron model requires n and $p+^{12}$C potentials at half the incident deuteron energy, i.e., 7.5 and 15 MeV for the calculations at 15 and 30 MeV, respectively. Three different sets of potentials were used, viz. empirical optical model potentials obtained by fitting the appropriate n and $p+^{12}$C elastic scattering data, potentials calculated using the global parametrization of Watson *et al.* [32] for nucleon scattering from $1p$-shell nuclei, and potentials calculated using the JLM prescription [33–36]. All JLM potentials used in this work have an imaginary potential normalization factor $\lambda=0.8$, as used by Petler *et al.* [37] in their analysis of proton scattering from light targets. The empirical optical potentials were of Woods-Saxon form for the real part and Woods-Saxon derivative for the imaginary part. The parameters for an incident nucleon energy of 7.5 MeV are given in Table I.

For an incident nucleon energy of 15 MeV the $p+^{12}$C parameters were those of Nodvik *et al.* [38] and the $n+^{12}$C parameters were those of Spaargaren and Jonker [30], both minus the spin-orbit part. The ^{12}C density used to calculate the JLM potentials was the two-parameter Fermi function of El-Azab Farid and Satchler [39]. The spin-orbit parts of the JLM and Watson *et al.* potentials were also omitted, as the folding procedure used does not currently incorporate noncentral components of the nucleon-target potentials. This omission has a negligible effect on the cross sections.

Excitation of the ^{12}C 4.44 MeV 2^+ and 9.64 MeV 3^- states was included by deforming the bare Watanabe potential in the usual manner. Values for $B(E2;0^+\rightarrow 2^+)$ and $B(E3;0^+\rightarrow 3^-)$ were taken from Raman *et al.* [40] and Spear [41], respectively. Nuclear deformation lengths were extracted from the $B(E2;0^+\rightarrow 2^+)$ and $B(E3;0^+\rightarrow 3^-)$ values assuming the collective model and a ^{12}C radius of $1.2\times 12^{1/3}$ fm.

The transfer component of the calculations was implemented in the conventional manner, using the post form of the CRC formalism. The full complex remnant term and nonorthogonality correction were included. The $n-p$ binding potential was again the Reid soft core, with the D-state component explicitly included. The $n+^{12}$C binding potentials were of Woods-Saxon form with a radius parameter of $1.25\times 12^{1/3}$ fm and diffuseness 0.65 fm, the depths being adjusted to give the correct binding energy.

Three different sets of $p+^{13}$C optical potentials for the exit channel were also used: empirical, Watson *et al.* [32] and JLM, and were employed with the corresponding

TABLE II. Spectroscopic factors for the $^{12}C/^{13}C$ overlap, taken from Vinh Mau [43]. The left-hand column denotes the ^{12}C core spin and the ℓ, j quantum numbers of the transferred neutron.

	$\frac{1}{2}1^-$	$\frac{1}{2}1^+$	$\frac{5}{2}1^+$
$0 \otimes j$	0.791	0.957	0.867
$2 \otimes s_{1/2}$			0.179
$2 \otimes p_{3/2}$	0.602		
$2 \otimes d_{5/2}$		0.291	0.300
$3 \otimes p_{1/2}$			0.140
$3 \otimes p_{3/2}$			−0.326
$3 \otimes d_{5/2}$	0.111		

nucleon $+^{12}C$ potentials for the sake of consistency. The empirical potential parameters for the calculation at an incident deuteron energy of 15 MeV were obtained by fitting the data of Weller *et al.* [24] and are given in Table I. For the calculations at an incident deuteron energy of 30 MeV parameter set *B* of Greaves *et al.* [25] was used. The JLM potentials were calculated using two-parameter Fermi functions for the ^{13}C neutron and proton matter densities adjusted to have root-mean-square radii in agreement with those given in Satchler and Love [42]. All $p+^{13}C$ optical potentials retained the spin-orbit term.

Two-step transfer paths via the 4.44 MeV 2^+ and 9.64 MeV 3^- states of ^{12}C were also included in the calculations. Spectroscopic amplitudes ($\sqrt{C^2S}$, where S is the spectroscopic factor and C is the isospin Clebsch-Gordan coefficient, equal to 1.0 here) were taken from the calculations of Vinh Mau [43]. For ease of reference the values are given in Table II.

Transfers leading to the 0.0 MeV $1/2^-_1$, 3.09 MeV $1/2^+_1$, and 3.85 MeV $5/2^+_1$ states of ^{13}C were included in the calculations.

Before comparing the results of the calculations with the $d+^{12}C$ elastic and inelastic scattering and $^{12}C(d,p)^{13}C$ transfer data we present the predicted angular distributions together with the data for $p,n+^{12}C$ elastic scattering at 7.5 MeV (Fig. 1) and 15 MeV (Fig. 2) and $p+^{13}C$ elastic scattering at 16.75 MeV [Fig. 3(a)] and 30.4 MeV [Fig. 3(b)].

One may note that in general the nucleon scattering data at 7.5 MeV are not well described by either the Watson *et al.* [32] or the JLM potentials. Tests revealed that this is not due to the omission of their respective spin-orbit components, as their addition produced only minor changes to the predicted angular distributions. The 16.75 MeV $p+^{13}C$ data are also rather poorly described by the Watson *et al.* and JLM potentials, with the Watson *et al.* potential providing a somewhat better match to the data than the JLM potential.

By contrast, the nucleon scattering data at 15 MeV are rather well described by both Watson *et al.* and JLM potentials, with the latter giving the better description of the two. This is also true of the 30.4 MeV $p+^{13}C$ data, although the agreement between the Watson *et al.* potential prediction and the data is much poorer.

The poor agreement between the Watson *et al.* and JLM potential predictions and the data at the lower energies is not surprising, as the incident energy is rather lower than their strict range of validity. The JLM predictions of Petler *et al.* [37] are of similar quality at comparable incident energies. The 7.5 MeV $n+^{12}C$ data were difficult to describe satisfactorily even with an adjusted empirical optical potential. For the higher incident energies the agreement is much better, as might be expected. Overall, the JLM potentials provide a rather better description of the nucleon scattering data than the global parameters of Watson *et al.* [32].

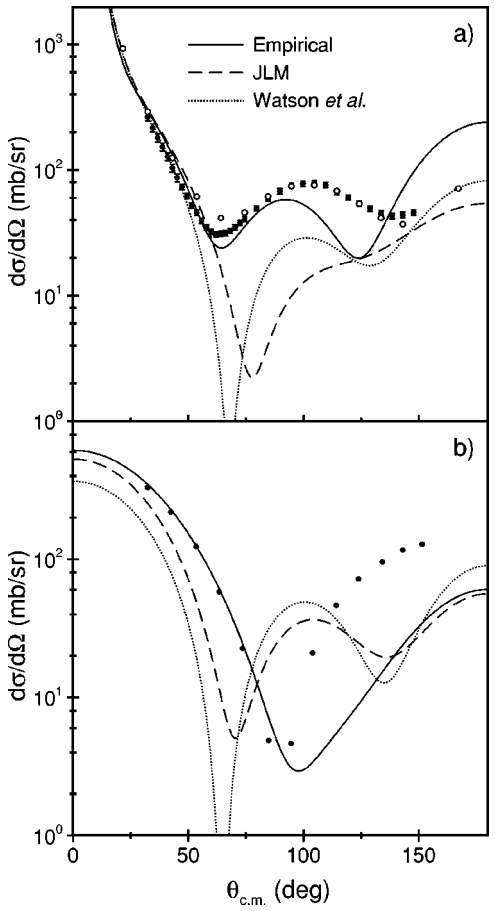

FIG. 1. Optical model predictions compared to data for $p+^{12}C$ (a) and $n+^{12}C$ (b) elastic scattering at 7.5 MeV. The $p+^{12}C$ data are from Sydow *et al.* [26] (filled circles) and Moss and Haeberli [27] (open circles) while the neutron data are from McDaniel *et al.* [29].

Calculations using the empirical and JLM potentials are compared to the $d+^{12}C$ elastic and inelastic scattering and $^{12}C(d,p)^{13}C$ data for an incident deuteron energy of 15 MeV in Figs. 4 and 5. Calculations using the Watson *et al.* [32] potentials give similar results to those using the JLM potentials.

In each case the depths of the real and imaginary parts of the bare Watanabe $d+^{12}C$ potentials were adjusted in order to obtain reasonable agreement with the measured $d+^{12}C$ elastic scattering angular distribution for the calculations including all the couplings. Normalization factors $N_R=1.0$, $N_I=0.7$; $N_R=1.0$, $N_I=0.6$; and $N_R=1.0$, $N_I=0.6$ were employed for the calculations using the empirical, Watson *et al.* [32] and JLM potentials, respectively. All calculations in-

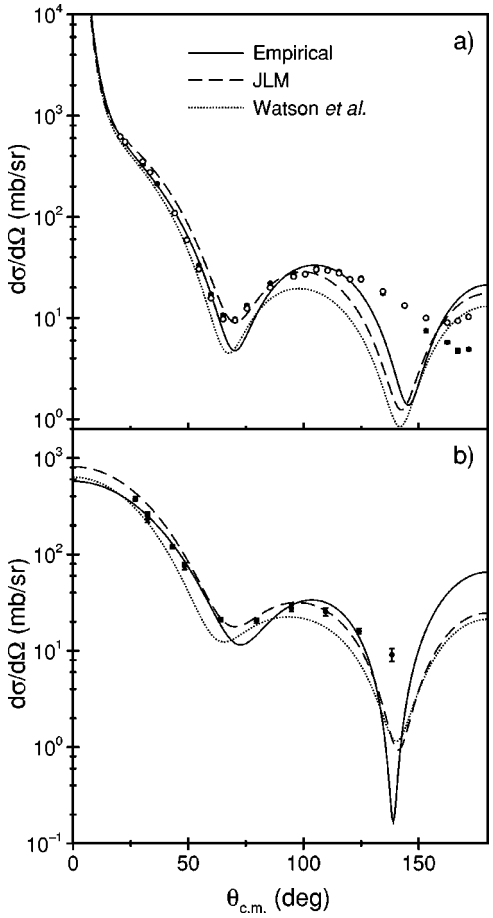

FIG. 2. Optical model predictions compared to data for $p+{}^{12}\mathrm{C}$ (a) and $n+{}^{12}\mathrm{C}$ (b) elastic scattering at 15 MeV. The $p+{}^{12}\mathrm{C}$ data are from Peelle *et al.* [28] for proton energies of 14.7 MeV (filled circles) and 15.2 MeV (open circles) while the neutron data are from Spaargaren and Jonker [30].

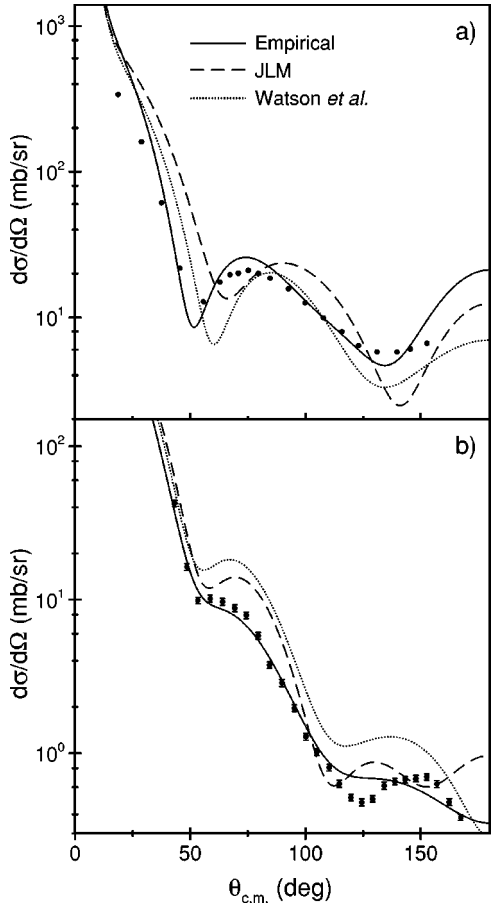

FIG. 3. Optical model predictions compared to data for $p+{}^{13}\mathrm{C}$ elastic scattering at 16.75 MeV (a) and 30.4 MeV (b). The data are from Weller *et al.* [24] and Greaves *et al.* [25], respectively.

cluded couplings to the 4.44 MeV 2^+ and 9.64 MeV 3^- states of $^{12}\mathrm{C}$ and part of the renormalization factors can be put down to this fact, as the effects of inelastic excitation of the $^{12}\mathrm{C}$ target are already included in the model in a broad sense via the $n,p+{}^{12}\mathrm{C}$ optical potentials.

Agreement with the elastic scattering data is rather good, that of the calculations using the empirical $n,p+{}^{12}\mathrm{C}$ optical potentials being comparable with the optical model fit of Busch *et al.* [19]. Agreement with the inelastic scattering data to the 4.44 MeV 2^+ state of $^{12}\mathrm{C}$ is less good, the calculations being consistently smaller than the data. The predicted inelastic cross sections were found to be rather sensitive to the imaginary depth of the bare Watanabe $d+{}^{12}\mathrm{C}$ potentials, and an increase of the nuclear deformation length would also lead to an increase in the predicted inelastic cross section. However, we have chosen not to optimize the fit to the 2^+ inelastic data as the transfer results are rather insensitive to it, and we wished to keep the excitation of the $^{12}\mathrm{C}$ 2^+ state on the same footing as that for the 3^- state, for which data are unavailable.

All the calculations agree on the negligible role played by transfer proceeding via the 9.64 MeV 3^- state of $^{12}\mathrm{C}$. This is understandable in view of the small spectroscopic amplitudes for these components given in Table I. There is also a reasonable agreement on the role of transfer proceeding by the $^{12}\mathrm{C}$ 4.44 MeV 2^+ state, although the details are somewhat dependent on the choice of input optical potentials. All the calculations agree that this process is only of significance for transfer to the 0.0 MeV $1/2^-$ state of $^{13}\mathrm{C}$, although the calculations using the Watson *et al.* [32] and JLM potentials assign a greater importance to it than those using the empirical potentials. The contribution of this transfer path to the 3.09 MeV $1/2^+$ and 3.85 MeV $5/2^+$ states of $^{13}\mathrm{C}$ is negligible for the calculations using the empirical and JLM potentials and small, but noticeable, for transfer to the $1/2^+$ state for those using the Watson *et al.* potentials.

Considered globally, we find that the results for transfer to the 3.09 MeV $1/2^+$ state are essentially insensitive to the input optical potentials, while those for transfer to the 0.0 MeV $1/2^-$ and 3.85 MeV $5/2^+$ states are rather more sensitive, particularly with regard to the magnitude of the forward angle cross sections. Given that the predicted forward angle transfer cross sections are unaffected by the addition of the two-step transfer paths, the calculations using the empirical optical potentials suggest that the $0^+\otimes j$ spectroscopic amplitudes of Vinh Mau [43] for the 0.0 MeV $1/2^-$ and 3.85 MeV $5/2^+$ states of $^{13}\mathrm{C}$ are too small. However, the forward angle cross sections for these states predicted by the

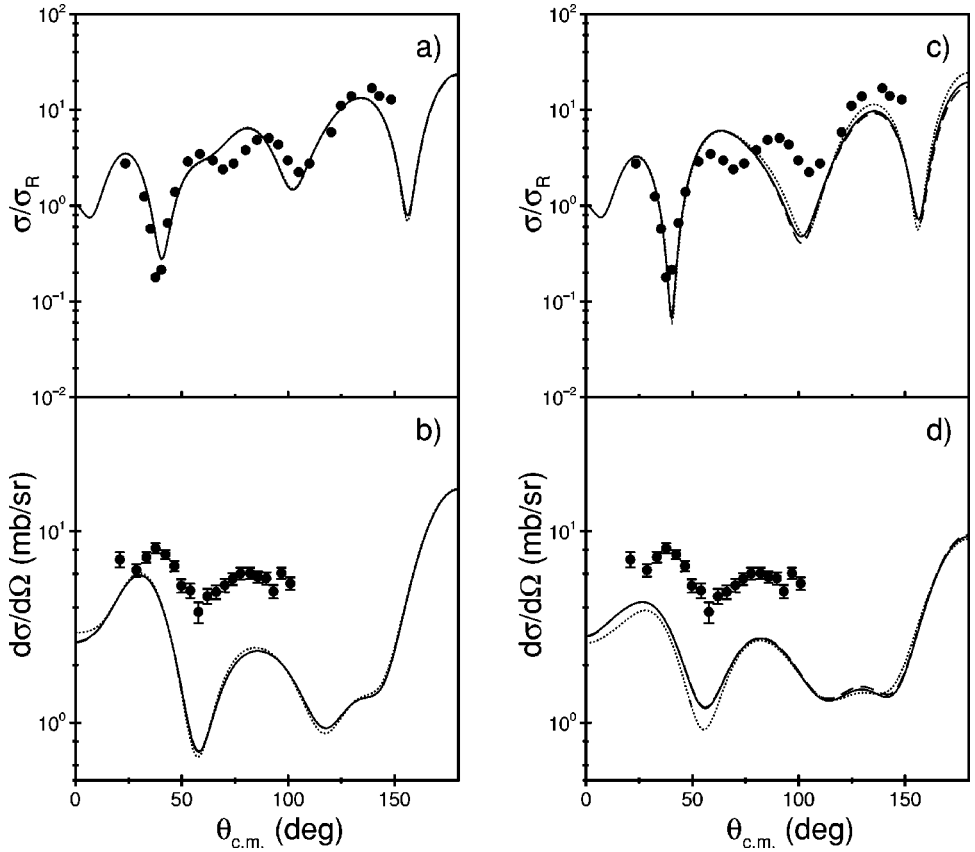

FIG. 4. Results of CDCC/CRC calculations at 15 MeV incident deuteron energy using empirical (a), (b) and JLM (c), (d) $p,n+{}^{12}\mathrm{C}$ and $p+{}^{13}\mathrm{C}$ potentials compared to $d+{}^{12}\mathrm{C}$ elastic and inelastic scattering data. The elastic scattering data (a), (c) are from Busch *et al.* [19] and the data for inelastic scattering to the 4.44 MeV 2^+ state of $^{12}\mathrm{C}$ (b), (d) from Haffner [21]. The solid, dashed, and dotted curves denote the results of the full calculation, the calculation omitting transfers via the 9.64 MeV 3^- state of $^{12}\mathrm{C}$, and the calculation omitting transfers via both the 9.64 MeV 3^- and 4.44 MeV 2^+states, respectively.

calculations using the Watson *et al.* and JLM potentials suggest that they are only slightly too small.

To summarize, consistent values for the forward angle cross sections are obtained from all the calculations for transfer to the 3.09 MeV $1/2^+$ state of $^{13}\mathrm{C}$, while for transfers to the 0.0 MeV $1/2^-$ and 3.85 MeV $5/2^+$ states the calculations using the Watson *et al.* [32] and JLM potentials give consistent values while the calculation using the empirical potentials gives rather smaller values. A test calculation using the JLM potentials to calculate the $d+{}^{12}\mathrm{C}$ potential in the entrance channel but with the empirical $p+{}^{13}\mathrm{C}$ potential in the exit channel found that the predicted angular distribution for transfer to the $5/2^+$ state was unaffected while that for transfer to the $1/2^-$ state was only affected at angles greater than the first peak of the angular distribution.

Calculations using the empirical and JLM potentials are compared to the $d+{}^{12}\mathrm{C}$ elastic and inelastic scattering and $^{12}\mathrm{C}(d,p)^{13}\mathrm{C}$ transfer data for an incident deuteron energy of 30 MeV in Figs. 6 and 7. Calculations using the Watson *et al.* [32] potentials give similar results to those using the JLM potentials.

The calculations were similar to those at 15 MeV incident deuteron energy. The depths of the real and imaginary parts of the bare Watanabe $d+{}^{12}\mathrm{C}$ potentials were again adjusted in order to obtain reasonable agreement with the measured $d+{}^{12}\mathrm{C}$ elastic scattering angular distribution for the calculations including all the couplings. Normalization factors $N_R=0.9$, $N_I=0.7$; $N_R=1.0$, $N_I=0.5$; and $N_R=1.0$, $N_I=0.7$ were employed for the calculations using the empirical, Watson *et al.* [32] and JLM potentials, respectively.

Agreement with the $d+{}^{12}\mathrm{C}$ elastic scattering data is good for all three calculations, somewhat better than that at 15 MeV. The agreement with the inelastic scattering data is notably better than at 15 MeV, although the calculations again consistently underestimate the data, particularly at the larger angles. The same comments regarding the sensitivity to the imaginary part of the bare Watanabe potential and increasing the nuclear deformation length as made for the calculations at 15 MeV also apply here.

One may draw similar conclusions regarding the importance of the two-step transfer processes as for the calculations at 15 MeV. Transfer proceeding via the 9.64 MeV 3^- state of $^{12}\mathrm{C}$ is again negligible, while that via the 4.44 MeV 2^+ state is only of significance for transfer leading to the 0.0 MeV $1/2^-$ state of $^{13}\mathrm{C}$. There is a slightly greater effect from paths proceeding via the $^{12}\mathrm{C}$ 2^+ state for transfers leading to the 3.09 MeV $1/2^+$ and 3.85 MeV $5/2^+$ than at 15 MeV, but it is still small compared to the direct transfer contribution, as might be expected from the spectroscopic amplitudes given in Table I.

Overall, one finds greater consistency between the calculations using different input potentials at 30 MeV than one does at 15 MeV. All the calculations give consistent values for the forward angle cross sections for all three states, although the details of the angular distributions show slight variations with input potential. This may indicate that for the higher energy the transfer cross sections are less sensitive to the details of the potentials used, or it may be merely indicative of the fact that the three sets of potentials predict similar $p,n+{}^{12}\mathrm{C}$ and $p+{}^{13}\mathrm{C}$ angular distributions (see Figs. 2 and 3).

The spectroscopic amplitudes of Vinh Mau [43] provide a reasonably good description of transfer to the 0.0 MeV $1/2^-$

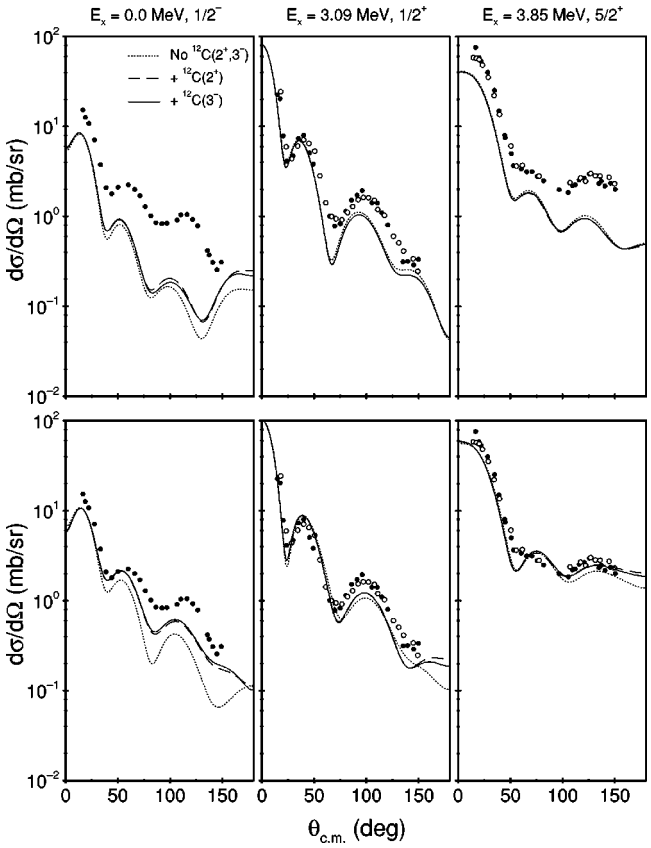

FIG. 5. Results of CDCC/CRC calculations at 15 MeV incident deuteron energy using empirical (upper panels) and JLM (lower panels) $p,n+{}^{12}\mathrm{C}$ and $p+{}^{13}\mathrm{C}$ potentials compared to the ${}^{12}\mathrm{C}(d,p){}^{13}\mathrm{C}$ transfer data of Darden *et al.* [16] (filled circles) and Hosono *et al.* [17] (open circles). The solid, dashed, and dotted curves denote the results of the full calculation, the calculation omitting transfers via the 9.64 MeV 3^- state of ${}^{12}\mathrm{C}$, and the calculation omitting transfers via both the 9.64 MeV 3^- and 4.44 MeV 2^+states, respectively.

and 3.09 MeV $1/2^+$ states of ${}^{13}\mathrm{C}$. However, although the magnitude of the forward angle cross section for transfer to the 3.85 MeV $5/2^+$ state is better reproduced than at 15 MeV, the shape of the angular distribution is rather poorly described, all three calculations considerably overpredicting the cross section for angles greater than about 25° in the center of mass frame.

To summarize, our method is able to describe rather well the ensemble of data for the ${}^{12}\mathrm{C}(d,p){}^{13}\mathrm{C}$ reaction at incident energies of 15 and 30 MeV, with the exception of that for inelastic scattering to the 4.44 MeV 2^+ state of ${}^{12}\mathrm{C}$ at an incident deuteron energy of 15 MeV. This is most likely due to difficulties with the input nucleon $+{}^{12}\mathrm{C}$ potentials at this rather low incident energy. The method enables the inclusion of two-step transfer paths proceeding via the excited states of ${}^{12}\mathrm{C}$ in a natural way, thus providing an excellent means of testing calculated spectroscopic amplitudes such as those of Vinh Mau [43]. Greater consistency between calculations using different input potentials is obtained at 30 MeV. In the following section the method will be applied to data for the ${}^{10}\mathrm{Be}(d,p){}^{11}\mathrm{Be}$ transfer reaction at incident deuteron energies of 12 and 25 MeV as an example of its application to radioactive nuclei.

III. CALCULATIONS FOR THE ${}^{10}\mathrm{Be}(d,p){}^{11}\mathrm{Be}$ SYSTEM

The structure of the ${}^{11}\mathrm{Be}$ nucleus provides a particularly interesting field of study, as in addition to being the archetype of a one neutron halo nucleus [44] it also exhibits a ground state spin-parity of $1/2^+$, rather than the $1/2^-$ predicted by the standard ordering of the shell model single particle levels. Various models of ${}^{11}\mathrm{Be}$ indicate a more or less important contribution from coupling of the single valence neutron to the 2_1^+ excited state of the deformed ${}^{10}\mathrm{Be}$ core in order to reproduce the observed ${}^{11}\mathrm{Be}$ ground state spin-parity; Winfield *et al.* [45] provide a useful summary of the relative contributions of the ${}^{10}\mathrm{Be}$ 0_1^+ and 2_1^+ states to the ${}^{11}\mathrm{Be}$ ground state predicted by many of these models. Values for the 2_1^+ contribution range from about 10% to about 40%; the majority of the calculations agree on a value of about 20%. While theoretical studies have concentrated on the ground state, it is also of interest to investigate the importance of coupling the valence neutron to the ${}^{10}\mathrm{Be}$ 2_1^+ state for the excited states of ${}^{11}\mathrm{Be}$. The ${}^{10}\mathrm{Be}(d,p)$ reaction provides a useful tool for such a study.

Data for the ${}^{10}\mathrm{Be}(d,p){}^{11}\mathrm{Be}$ reaction are available at incident deuteron energies of 12 MeV for transfers leading to the 0.0 MeV $1/2_1^+$ and the 0.32 MeV $1/2_1^-$ states of ${}^{11}\mathrm{Be}$ [46] and 25 MeV for transfer to the $1/2_1^+$, $1/2_1^-$ and 1.78 MeV $5/2_1^+$ states [47]. While the $5/2^+$ assignment for the ${}^{11}\mathrm{Be}$ 1.78 MeV state is not definitive [48], only the $\ell=2$ value being determined experimentally [47], we have followed the majority of structure calculations in assigning it this value.

Unfortunately, nucleon $+{}^{10}\mathrm{Be}$ elastic scattering data do not exist at suitable energies for calculations at 12 MeV. However, $p+{}^{10}\mathrm{Be}$ data exist at incident proton energies of 12 and 13 MeV [46], suitable for the calculations at an incident deuteron energy of 25 MeV. Data for $p+{}^{11}\mathrm{Be}$ elastic scattering are also not available at suitable energies. Deuteron $+{}^{10}\mathrm{Be}$ elastic scattering data over a very limited angular range are available at 12 MeV [46], there being none available for an incident energy of 25 MeV. No data for $d+{}^{10}\mathrm{Be}$ inelastic scattering exist. Thus, for the ${}^{10}\mathrm{Be}(d,p){}^{11}\mathrm{Be}$ calculations the necessary input potentials must be provided by global systematics or calculations based on effective interactions such as the JLM.

The calculations were similar to those carried out for the $d+{}^{12}\mathrm{C}$ system, with the exception that the $n-p$ continuum was truncated at $k_{\max}=0.375\ \mathrm{fm}^{-1}$ for the calculations at 12 MeV, this being found sufficient at this energy. Two sets of $p,n+{}^{10}\mathrm{Be}$ and $p+{}^{11}\mathrm{Be}$ potentials were used, the Watson *et al.* [32] global parametrization and potentials calculated using the JLM prescription [33–36]. The JLM potentials again employed the imaginary potential normalization factor $\lambda=0.8$ of Petler *et al.* [37]. The ${}^{10}\mathrm{Be}$ and ${}^{11}\mathrm{Be}$ densities used to calculate the JLM potentials were taken from Sagawa [49]. The spin-orbit parts of the $p,n+{}^{10}\mathrm{Be}$ potentials were again omitted, this making little difference to the predicted elastic scattering. All $p+{}^{11}\mathrm{Be}$ potentials retained the spin-orbit term.

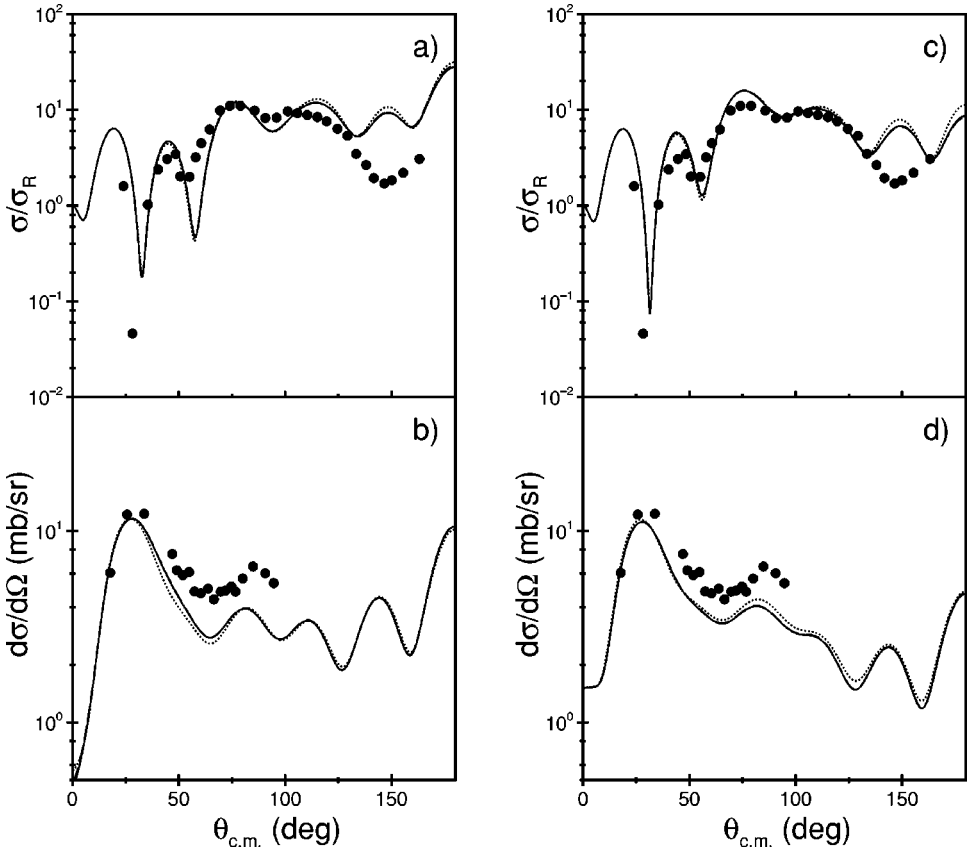

FIG. 6. Results of CDCC/CRC calculations at 30 MeV incident energy using empirical (a), (b) and JLM (c), (d) $p,n+{}^{12}$C and $p+{}^{13}$C potentials compared to $d+{}^{12}$C elastic and inelastic scattering data. The elastic scattering data (a), (c) are from Perrin *et al.* [20] and the data for inelastic scattering to the 4.44 MeV 2^+ state of ^{12}C (b), (d) from Lind *et al.* [22] and Kubo *et al.* [23]. The solid, dashed, and dotted curves denote the results of the full calculation, the calculation omitting transfers via the 9.64 MeV 3^- state of ^{12}C, and the calculation omitting transfers via both the 9.64 MeV 3^- and 4.44 MeV 2^+ states, respectively.

As noted in Auton [46], the Watson *et al.* potential provides a good description of the $p+{}^{10}$Be elastic scattering data at incident proton energies of 12–16 MeV. The JLM potential gives a similar quality fit to the data at 12–13 MeV, the appropriate energy for the calculations at an incident deuteron energy of 25 MeV. Both Watson *et al.* and JLM potentials predict similar elastic scattering angular distributions for $n+{}^{10}$Be at 12.5 MeV and $p+{}^{11}$Be at approximately 21 MeV, also required for the 25 MeV calculations. For the calculations at an incident deuteron energy of 12 MeV, the Watson *et al.* and JLM potentials predict similar $p+{}^{11}$Be elastic scattering, while the predicted $p,n+{}^{10}$Be elastic scattering angular distributions exhibit a rather larger difference depending on the potential used than for the calculations at an incident nucleon energy of 12.5 MeV.

Excitation of the 3.37 MeV 2^+ state of ^{10}Be was included by deforming the bare Watanabe potential, the $B(E2;0^+ \rightarrow 2^+)$ being taken from Raman *et al.* [40]. For the nuclear deformation length we adopted a different approach to that used for ^{12}C, taking the value obtained by Iwasaki *et al.* [50] from a proton scattering analysis. This gives a slightly smaller value than that extracted from the $B(E2)$ using the collective model and a ^{10}Be radius of $1.2\times10^{1/3}$ fm.

The transfer component of the calculations again included the full complex remnant term and nonorthogonality correction. Transfers to the 0.0 MeV $1/2^+_1$, 0.32 MeV $1/2^-_1$, and 1.78 MeV $5/2^+_1$ states in ^{11}Be were included. The $n-p$ binding potential was the Reid soft core, with the D-state component explicitly included, and the $n+{}^{10}$Be binding potentials were of Woods-Saxon form with a radius parameter of $1.25\times10^{1/3}$ fm and diffuseness 0.65 fm. The depth of the $n+{}^{10}$Be potentials was adjusted to give the correct binding energy for the $1/2^+_1$ and $1/2^-_1$ states. The $5/2^+_1$ state, being unbound, was treated as a resonant bin of width $\Delta E=0.5$ MeV, with the depth of the $n+{}^{10}$Be potential being adjusted to give a resonance at the correct energy. The $n+{}^{10}$Be wave function was calculated out to a radius of 100 fm; test calculations using a radius of 200 fm yielded the same results, indicating that truncation at 100 fm is sufficient.

Two-step transfer paths via the 3.37 MeV 2^+ state of ^{10}Be were also included. Spectroscopic amplitudes were again taken from the calculations of Vinh Mau [43]. For ease of reference the values are given in Table III.

Calculations using both sets of input potentials are compared to the ^{10}Be$(d,p)^{11}$Be transfer data at an incident deuteron energy of 12 MeV in Fig. 8.

In each case the depths of the real and imaginary parts of the bare Watanabe $d+{}^{10}$Be potentials were adjusted in order to obtain reasonable agreement between the $d+{}^{10}$Be elastic scattering angular distribution predicted by the calculations including all the couplings and that predicted by a calculation including the deuteron breakup effects only, there being essentially no elastic scattering data available. This procedure was adopted in order to avoid as much as possible "double counting" of effects due to the inelastic excitation of ^{10}Be. Normalization factors $N_R=1.0$, $N_I=0.4$ and $N_R=0.9$, $N_I=0.7$ were employed for the calculations using the Watson *et al.* [32] and JLM potentials, respectively.

Both sets of calculations give consistent values for the magnitude of the forward angle cross sections, as was found

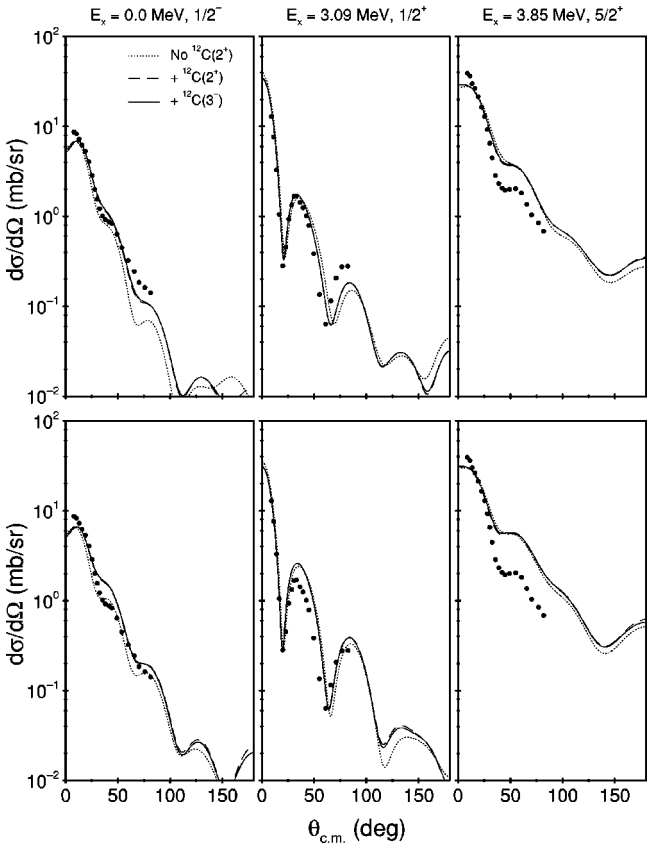

FIG. 7. Results of CDCC/CRC calculations at 30 MeV incident deuteron energy using empirical (upper panels) and JLM (lower panels) $p,n+{}^{12}\mathrm{C}$ and $p+{}^{13}\mathrm{C}$ potentials compared to the ${}^{12}\mathrm{C}(d,p){}^{13}\mathrm{C}$ transfer data of Ohnuma *et al.* [18]. The solid, dashed, and dotted curves denote the results of the full calculation, the calculation omitting transfers via the 9.64 MeV 3^- state of ${}^{12}\mathrm{C}$, and the calculation omitting transfers via both the 9.64 MeV 3^- and 4.44 MeV 2^+ states, respectively.

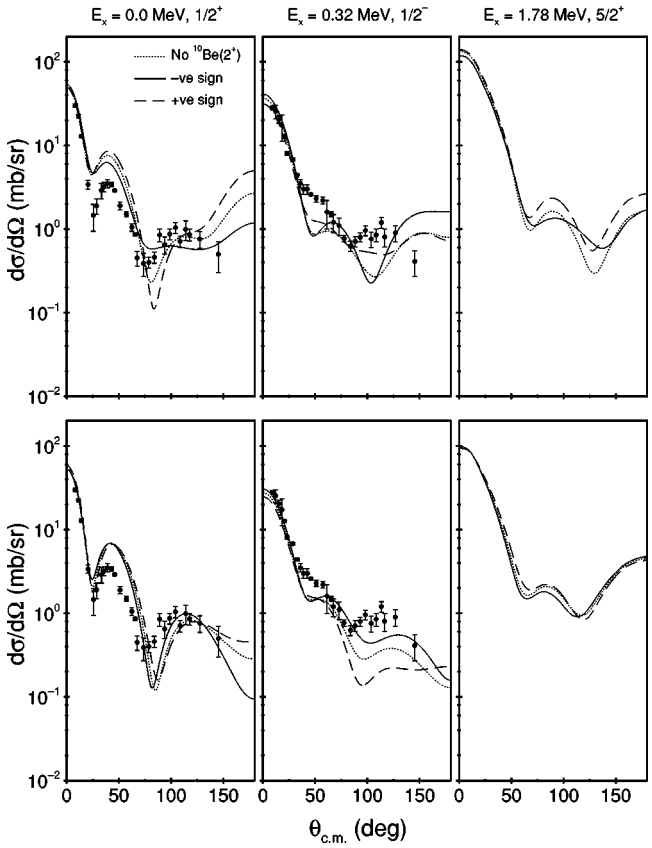

FIG. 8. Results of CDCC/CRC calculations at 12 MeV incident deuteron energy using Watson *et al.* [32] (upper panels) and JLM (lower panels) $p,n+{}^{10}\mathrm{Be}$ and $p+{}^{11}\mathrm{Be}$ potentials compared to the ${}^{10}\mathrm{Be}(d,p){}^{11}\mathrm{Be}$ transfer data of Auton [46]. The solid, dashed, and dotted curves denote the results of the full calculation with negative relative sign between the spectroscopic factors for the ${}^{11}\mathrm{Be}/{}^{10}\mathrm{Be}(0^+)$ and ${}^{11}\mathrm{Be}/{}^{10}\mathrm{Be}(2^+)$ overlaps, the full calculation with positive relative sign between the spectroscopic factors for the ${}^{11}\mathrm{Be}/{}^{10}\mathrm{Be}(0^+)$ and ${}^{11}\mathrm{Be}/{}^{10}\mathrm{Be}(2^+)$ overlaps and the calculation omitting transfers via the 3.37 MeV 2^+ state, respectively.

for the ${}^{12}\mathrm{C}(d,p){}^{13}\mathrm{C}$ calculations at 15 MeV incident deuteron energy using the Watson *et al.* and JLM potentials. The agreement with data for transfer to the 0.0 MeV $1/2^+$ and 0.32 MeV $1/2^-$ states of ${}^{11}\mathrm{Be}$ is reasonable (there are no data available for transfer to the 1.78 MeV $5/2^+$ state at 12 MeV incident deuteron energy) with the forward angle magnitude of the cross sections being well described by the spectroscopic amplitudes of Vinh Mau [43]. Two-step transfer via the 3.37 MeV 2^+ state of ${}^{10}\mathrm{Be}$ has little effect on any of the predicted angular distributions for angles smaller than about 75° in the center of mass frame.

TABLE III. Spectroscopic factors for the ${}^{10}\mathrm{Be}/{}^{11}\mathrm{Be}$ overlap, taken from Vinh Mau [43]. The left-hand column denotes the ${}^{10}\mathrm{Be}$ core spin and the ℓ,j quantum numbers of the transferred neutron.

	$\frac{1}{2}1^+$	$\frac{1}{2}1^-$	$\frac{5}{2}1^+$
$0\otimes j$	0.964	0.764	0.896
$2\otimes s_{1/2}$			0.269
$2\otimes p_{3/2}$		0.667	
$2\otimes d_{5/2}$	0.267		0.353

Following Zwieglinski *et al.* [47] we tested the effect of changing the relative sign of the spectroscopic amplitudes for the ${}^{11}\mathrm{Be}/{}^{10}\mathrm{Be}(0^+)$ and ${}^{11}\mathrm{Be}/{}^{10}\mathrm{Be}(2^+)$ overlaps (Vinh Mau [43] gives them as positive, see Table III). While the predicted cross sections at large angles are rather more sensitive to the sign than found by Zwieglinski *et al.* [47] at an incident deuteron energy of 25 MeV, the spread in cross section is comparable to that produced by using the different sets of input potentials, compare the solid and dashed curves in Fig. 8.

Overall, one may note that for an incident deuteron energy of 12 MeV the calculations are essentially insensitive to the two-step transfer path, in contrast to the 15 MeV ${}^{12}\mathrm{C}(d,p){}^{13}\mathrm{C}$ calculations, where transfer to the 0.0 MeV $1/2^-$ state was found to be sensitive to the two-step mode proceeding via the 4.44 MeV 2^+ state of ${}^{12}\mathrm{C}$. This is somewhat surprising considering that the spectroscopic amplitudes of Vinh Mau have a ${}^{11}\mathrm{Be}/{}^{10}\mathrm{Be}(2^+)$ component for the 0.32 MeV $1/2^-$ state of ${}^{11}\mathrm{Be}$ of comparable size to that of the ${}^{11}\mathrm{Be}/{}^{10}\mathrm{Be}(0^+)$ one.

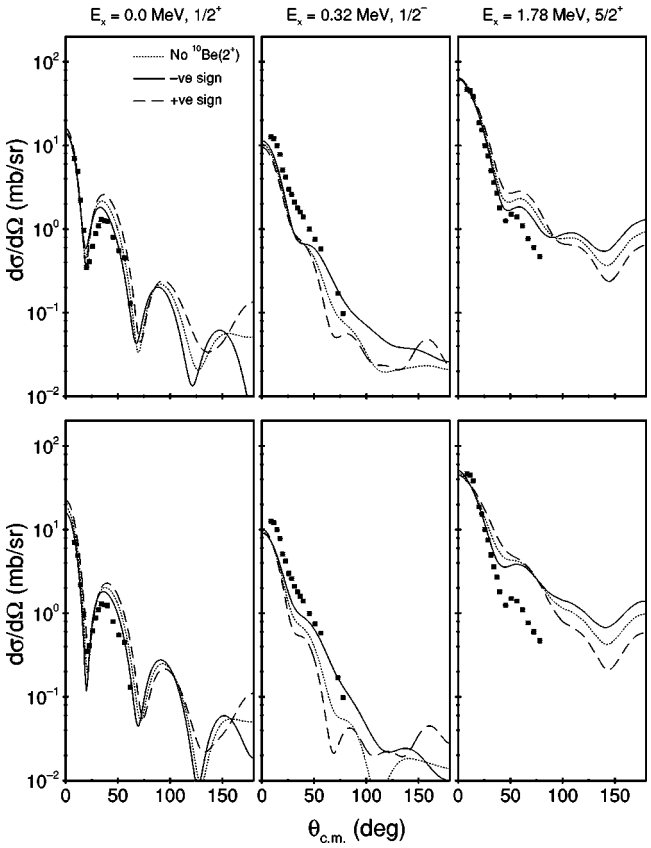

FIG. 9. Results of CDCC/CRC calculations at 25 MeV incident deuteron energy using Watson *et al.* [32] (upper panels) and JLM (lower panels) $p,n+{}^{10}$Be and $p+{}^{11}$Be potentials compared to the ${}^{10}\mathrm{Be}(d,p){}^{11}\mathrm{Be}$ transfer data of Zwieglinski *et al.* [47]. The solid, dashed, and dotted curves denote the results of the full calculation with negative relative sign between the spectroscopic factors for the ${}^{11}\mathrm{Be}/{}^{10}\mathrm{Be}(0^+)$ and ${}^{11}\mathrm{Be}/{}^{10}\mathrm{Be}(2^+)$ overlaps, the full calculation with positive relative sign between the spectroscopic factors for the ${}^{11}\mathrm{Be}/{}^{10}\mathrm{Be}(0^+)$ and ${}^{11}\mathrm{Be}/{}^{10}\mathrm{Be}(2^+)$ overlaps and the calculation omitting transfers via the 3.37 MeV 2^+ state, respectively.

Calculations using both sets of input potentials are compared to the ${}^{10}\mathrm{Be}(d,p){}^{11}\mathrm{Be}$ transfer data at an incident deuteron energy of 25 MeV in Fig. 9.

The calculations were similar to those at 12 MeV incident deuteron energy. The depths of the real and imaginary parts of the bare Watanabe $d+{}^{10}$Be potentials were again adjusted in order to obtain reasonable agreement between the $d+{}^{10}$Be elastic scattering angular distribution predicted by the calculations including all the couplings and that predicted by a calculation including the deuteron breakup effects only, there being no elastic scattering data available at this energy. Normalization factors $N_R=1.0$, $N_\mathrm{I}=0.6$ and $N_R=1.0$, $N_\mathrm{I}=0.6$ were employed for the calculations using the Watson *et al.* [32] and JLM potentials, respectively.

Again, one may note the relative insensitivity to the two-step transfer proceeding via the 3.37 MeV 2^+ state of ^{10}Be for angles forward of about 50° in the center of mass frame, although the degree of sensitivity is somewhat dependent on the choice of potentials used. Both sets of potentials again yield consistent forward angle cross section magnitudes, with the details of the angular distributions varying slightly for the two sets of potentials. The largest difference in the predicted angular distributions is for transfer to the 1.78 MeV $5/2^+$ state, the Watson *et al.* [32] potentials yielding a better description of the angular distribution for angles greater than about 30° in the center of mass frame.

We again tested the effect of changing the relative sign between the spectroscopic amplitudes for the ${}^{10}\mathrm{Be}(0^+)/{}^{11}\mathrm{Be}$ and ${}^{10}\mathrm{Be}(2^+)/{}^{11}\mathrm{Be}$ overlaps. We found a slightly larger sensitivity to the sign than in the CCBA calculations of Zwieglinski *et al.* [47] for the same data, with a definite preference for a relative negative sign for the 0.0 MeV $1/2^+$ and 1.78 MeV $5/2^+$ states, compare the solid and dashed curves in Fig. 9. It is less clear for the 0.32 MeV $1/2^-$ state which sign is preferred, as the magnitude of the forward angle cross section is not well reproduced by the spectroscopic amplitudes of Vinh Mau [43] for this state. However, if the ${}^{10}\mathrm{Be}(0^+)/{}^{11}\mathrm{Be}$ component were increased to match the data a positive relative sign between the two components would give the best agreement.

Overall, the spectroscopic amplitudes of Vinh Mau [43] provide a reasonable description of the data for transfer to the 0.0 MeV $1/2^+$ and 1.78 MeV $5/2^+$ states. However, in contrast to the results for an incident deuteron energy of 12 MeV, the magnitude of the forward angle cross section for transfer to the 0.32 MeV $1/2^-$ state is poorly described. Both sets of potentials suggest that the spectroscopic factor of Vinh Mau [43] for the ${}^{10}\mathrm{Be}(0^+)/{}^{11}\mathrm{Be}$ overlap for this state is too small. Other calculations, by Nunes *et al.* [51] and Bhattacharya and Krishan [52], which yield spectroscopic amplitudes of 0.93 and 1.00, respectively, for this component of the ^{11}Be 0.32 MeV $1/2^-$ state support this conclusion. Given that both sets of input potentials are outside their strict energy range of validity for the calculations for an incident deuteron energy of 12 MeV, one would expect the results for 25 MeV deuteron energy to be more reliable. However, without the relevant $d+{}^{10}$Be and $p+{}^{11}$Be elastic scattering data it is impossible to draw firm conclusions on this point.

We also note a similar problem with the description of transfer to the 1.78 MeV $5/2^+$ state of ^{11}Be to that found for transfer to the 3.85 MeV $5/2^+$ state of ^{13}C at an incident deuteron energy of 30 MeV. While the magnitude of the forward angle cross section is well reproduced, at larger angles the calculated cross section considerably overpredicts the data, the exact extent of this overprediction being dependent on the input potentials used.

To summarize the calculations for the ${}^{10}\mathrm{Be}(d,p){}^{11}\mathrm{Be}$ transfer reaction, at each energy both sets of potentials give consistent results *at that energy*. However, the calculated cross sections for transfer to the 0.32 MeV $1/2^-$ state of ^{11}Be at an incident deuteron energy of 25 MeV noticeably underpredict the data, in contrast to the result for an incident deuteron energy of 12 MeV. Similar problems were found with regard to the description of transfer to the 1.78 MeV $5/2^+$ state of ^{11}Be at an incident deuteron energy of 25 MeV to those for transfer to the 3.85 MeV $5/2^+$ state of ^{13}C at an incident deuteron energy of 30 MeV, although the exact extent of the problem is more sensitive to the potentials used for the ${}^{10}\mathrm{Be}(d,p){}^{11}\mathrm{Be}$ transfer than for ${}^{12}\mathrm{C}(d,p){}^{13}\mathrm{C}$.

As discussed above, the calculations for an incident deuteron energy of 25 MeV are expected to be more realistic.

The discrepancy between the calculated and measured cross sections for transfer to the 0.32 MeV $1/2^-$ state could be due to the spectroscopic amplitude of Vin Mau [43] being too small, as noted above. However, Timofeyuk and Johnson [53] have performed adiabatic model calculations for transfer to the 0.0 MeV $1/2^+$ state of ^{11}Be at 25 MeV incident deuteron energy in which ^{11}Be breakup was included in an approximate way, and found that its inclusion increased the transfer cross section. As we have not included ^{11}Be breakup effects in our calculations this is a possible alternative explanation. Test calculations that included the dipole coupling between the 0.0 MeV $1/2^+$ and 0.32 MeV $1/2^-$ states of ^{11}Be found that it had no effect on the transfer cross sections, despite the large $B(E1)$ value for this transition, due to the small charge product of the system.

IV. CONCLUSIONS

We have presented a comprehensive analysis method for (d,p) reactions that brings together existing elements from the literature to produce a calculation that includes all important physical effects on the same footing and as accurately as possible. The method was tested against data for the ^{12}C$(d,p)^{13}$C reaction, including the relevant elastic and inelastic scattering, and found to be able to provide a reasonably good simultaneous description of all the data at two different incident deuteron energies.

Three different sets of input potentials were tested for each deuteron energy: empirical potentials obtained from fits to the relevant nucleon elastic scattering data, the global parametrization for 1*p*-shell nuclei of Watson *et al.* [32] and potentials calculated using the JLM effective interaction. Greater consistency between the results using the three sets of potentials was found at the higher deuteron incident energy, 30 MeV, while overall better consistency was obtained between the calculations using the Watson *et al.* and JLM potentials. This latter effect is similar to that noted by Liu *et al.* [54] in their extensive reanalysis of ^{12}C$(d,p)^{13}$C and ^{13}C$(p,d)^{12}$C ground-state to ground-state transfers.

The method was then used to analyze data for the ^{10}Be$(d,p)^{11}$Be transfer at two similar incident deuteron energies, 12 and 25 MeV, where suitable elastic scattering data do not exist. Calculations were performed using the Watson *et al.* and JLM potentials as input, and produced consistent results *at a given energy* for both potentials. However, when the results for transfer to the 0.32 MeV $1/2^-$ state of ^{11}Be at 12 and 25 MeV incident deuteron energy were compared an inconsistency was found. The calculations at 25 MeV significantly underestimated the data, suggesting that the spectroscopic amplitudes used, those of Vinh Mau [43], were too small, whereas at 12 MeV the data were rather well described. This discrepancy could be due to neither set of input potentials being realistic for an incident deuteron energy of 12 MeV (the energies being too low for the range of validity of either the Watson *et al.* or JLM potentials) or to the effects of the breakup of ^{11}Be, not included in the calculations. Without the necessary elastic scattering data (entrance channel $d+^{10}$Be and exit channel $p+^{11}$Be) it is impossible to draw firm conclusions on this point.

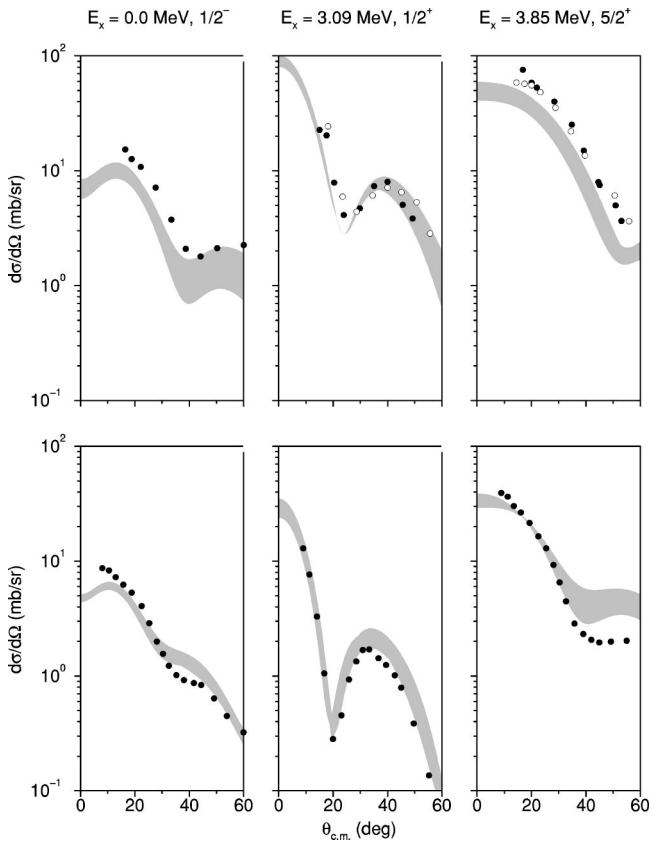

FIG. 10. Results of CDCC/CRC calculations at 15 MeV (upper panels) and 30 MeV (lower panels) incident deuteron energy compared to the forward angle ^{12}C$(d,p)^{13}$C transfer cross sections. The shaded areas indicate the uncertainty in the differential cross sections predicted by calculations using the three sets of input potentials.

We may draw some general conclusions from the calculations presented here that may be of use for future experiments concerned with (d,p) reactions using radioactive beams in inverse kinematics. In order to carry out a meaningful analysis the absolute minimum additional data required besides the transfer cross section angular distributions are the angular distribution for deuteron elastic scattering at the same energy. It is also highly desirable to obtain the exit channel proton elastic scattering data at the appropriate energy. One may then use JLM potentials to provide basic input for the deuteron breakup part of the calculation, the real and imaginary parts of the bare Watanabe potential being adjusted so that the full calculation provides an optimum fit to the deuteron elastic scattering data. A JLM potential would also be used for the exit channel proton potential, and if the appropriate data were available its real and imaginary potential depths would be adjusted to obtain an optimum fit. In this way both entrance and exit channel parameters would be controlled by appropriate data.

We also conclude that data taken at an incident deuteron energy of around 30 MeV or higher would prove most useful. As demonstrated above, the calculations are less sensitive to the input potentials at this energy. This is well illustrated in Fig. 10, where the uncertainty in the ^{12}C$(d,p)^{13}$C forward angle cross sections predicted by the three sets of

input potentials is shown for incident deuteron energies of 15 MeV (upper panels) and 30 MeV (lower panels). As may be seen, the spread is much smaller for the higher incident energy, the predicted forward angle cross sections, and hence the spectroscopic factors that may be extracted from the data, being essentially independent of the choice of input optical potentials. In addition, the JLM potential provides good descriptions of nucleon scattering for stable nuclei in this energy regime, as do global parametrizations. At the lower energies investigated here there are also possible problems with resonances in the nucleon elastic scattering at the required energies, which will cause additional complications to the analysis and may be the reason for the rather poor description of the $d+^{12}$C inelastic scattering data at 15 MeV.

Test calculations for the ^{12}C(d,p) system found that at an incident deuteron energy of 15 MeV the effect of omitting the remnant term and nonorthogonality correction on the predicted elastic scattering was essentially negligible, while at 30 MeV incident deuteron energy the effect was only significant at backward angles. The effect on the predicted transfer angular distributions for both energies was essentially negligible for angles smaller than about 25° in the center of mass frame, smaller than the effect due to the use of different input optical potentials. For angles greater than 25° the effect was of comparable size to that due to the use of different input optical potentials. Thus, the use of the remnant term merely allows an arbitrary choice between the use of post or prior form for the transfer component of the calculation. The use of the post formulation without this correction for a stripping reaction gives essentially the same result, as expected for light ions.

Test calculations in which the deuteron breakup couplings were omitted found little change to either the predicted elastic scattering or transfer angular distributions for an incident deuteron energy of 15 MeV, the differences being at the level of those due to the use of different input optical potentials. At 30 MeV the effect on the predicted elastic and inelastic scattering of omitting the breakup couplings was significant. However, the predicted transfer angular distributions were essentially unchanged for angles smaller than approximately 20° in the center of mass frame, the effect at angles greater than this being comparable to that due to the use of different input optical potentials. This relatively small effect on the transfer cross sections of the deuteron breakup couplings may be ascribed to the small mass and charge of the target. For heavier targets a larger effect is expected and this will be investigated in future work. It should however be noted that in all cases the best description of the data was obtained when the remnant term, nonorthogonality correction and deuteron breakup couplings were included in the calculations.

To summarize our recommendations for future (d,p) experiments involving radioactive beams in inverse kinematics, our calculations suggest that data be taken at around 15 MeV per nucleon or higher incident energy and for angles out to approximately $30°-40°$ in the center of mass frame. The minimum additional data required for an unambiguous analysis are the deuteron elastic scattering at the appropriate energy, with the exit channel proton elastic scattering data being highly desirable if experimental constraints allow. Such data should allow a consistent determination of single neutron spectroscopic amplitudes, with the proviso that for weakly bound exotic residual nuclei in the exit channel the effects of breakup will need to be included in some way [53].

For the future, a deuteron static spin-orbit term could be added to the calculations, derived from the nucleon spin-orbit potentials. This would be necessary for an analysis of data taken with the polarized deuteron targets currently being contemplated for radioactive beam facilities, as the static spin-orbit potential is known to dominate the analyzing powers for polarized deuteron elastic scattering (this is illustrated very well in Rawitscher and Mukherjee [5], for example). This deuteron static spin-orbit potential could also have an influence on the analyzing powers for the (d,p) transfer reaction, an excellent observable for unambiguously determining the intrinsic spin of states, and thus needs to be included in a truly comprehensive analysis method.

The method may also be naturally extended to include (d,n) and (p,d) transfer reactions. The extension to (d,n) reactions is essentially trivial, as the outgoing proton is merely replaced by a neutron and a similar method has already been applied to the ^{7}Be$(d,n)^{8}$B reaction [55]. The application to (p,d) reactions should also be straightforward.

ACKNOWLEDGMENTS

The authors would like to thank Professor R. C. Johnson for useful discussions concerning the analysis of (d,p) reactions and Professor I. J. Thompson for help with technical aspects of the FRESCO calculations.

[1] R. C. Johnson and P. J. R. Soper, Phys. Rev. C **1**, 976 (1971).
[2] J. D. Harvey and R. C. Johnson, Phys. Rev. C **3**, 636 (1971).
[3] M. D. Cooper, W. F. Hornyak, and P. G. Roos, Nucl. Phys. **A218**, 249 (1974).
[4] G. H. Rawitscher, Phys. Rev. C **11**, 1152 (1974).
[5] G. H. Rawitscher and S. N. Mukherjee, Nucl. Phys. **A342**, 90 (1980).
[6] M. Yahiro, M. Nakano, Y. Iseri, and M. Kamimura, Prog. Theor. Phys. **67**, 1467 (1982).
[7] R. Y. Rasoanaivo and G. H. Rawitscher, Phys. Rev. C **39**, 1709 (1989).
[8] N. Austern, Y. Iseri, M. Kamimura, M. Kawai, G. Rawitscher, and M. Yahiro, Phys. Rep. **154**, 124 (1987).
[9] Y. Iseri, M. Yahiro, and M. Nakano, Prog. Theor. Phys. **69**, 1038 (1983).
[10] R. V. Reid, Jr., Ann. Phys. (N.Y.) **50**, 441 (1968).
[11] R. C. Johnson and F. D. Santos, Phys. Rev. Lett. **19**, 364 (1967).
[12] R. C. Brown, A. A. Debenham, G. W. Greenlees, J. A. R. Griffith, O. Karban, D. C. Kocher, and S. Roman, Phys. Rev.

Lett. **27**, 1446 (1971).
[13] R. C. Johnson, F. D. Santos, R. C. Brown, A. A. Debenham, G. W. Greenlees, J. A. R. Griffith, O. Karban, D. C. Kocher, and S. Roman, Nucl. Phys. **A208**, 221 (1973).
[14] N. Rohrig and W. Haeberli, Nucl. Phys. **A206**, 225 (1973).
[15] L. D. Knutson, E. J. Stephenson, N. Rohrig, and W. Haeberli, Phys. Rev. Lett. **31**, 392 (1973).
[16] S. E. Darden, S. Sen, H. R. Hiddleston, J. A. Aymar, and W. A. Yoh, Nucl. Phys. **A208**, 77 (1973).
[17] K. Hosono, J. Phys. Soc. Jpn. **25**, 36 (1968).
[18] H. Ohnuma, N. Hoshino, O. Mikoshiba, K. Raywood, A. Sakaguchi, G. G. Shute, B. M. Spicer, M. H. Tanaka, M. Tanifuji, T. Terasawa, and M. Yasue, Nucl. Phys. **A448**, 205 (1986).
[19] C. E. Busch, T. B. Clegg, S. K. Datta, and E. J. Ludwig, Nucl. Phys. **A223**, 183 (1974).
[20] G. Perrin, N. V. Sen, J. Arvieux, A. Fiore, J. L. Durand, R. Darves-Blanc, J. C. Gondrand, F. Merchez, and C. Perrin, Nucl. Phys. **A193**, 215 (1972).
[21] J. W. Haffner, Phys. Rev. **103**, 1398 (1956).
[22] J. M. Lind, G. T. Garvey, and R. E. Tribble, Nucl. Phys. **A276**, 25 (1977).
[23] K.-I. Kubo, K. Nagatani, and K. G. Nair, Phys. Rev. C **15**, 1758 (1977).
[24] H. R. Weller, J. Szücs, P. G. Ikossi, J. A. Kuehner, D. T. Petty, and R. G. Segler, Phys. Rev. C **18**, 1120 (1978).
[25] P. D. Greaves, V. Hnizdo, J. Lowe, and O. Karban, Nucl. Phys. **A179**, 1 (1972).
[26] L. Sydow, S. Vohl, P. Nießen, K. R. Nyga, R. Reckenfelderbäumer, G. Rauprich, and H. Paetz, Nucl. Instrum. Methods Phys. Res. A **327**, 441 (1993).
[27] S. J. Moss and W. Haeberli, Nucl. Phys. **72**, 417 (1965).
[28] R. W. Peelle, Phys. Rev. **105**, 1311 (1957).
[29] F. D. McDaniel, M. W. McDonald, M. F. Steuer, and R. M. Wood, Phys. Rev. C **6**, 1181 (1972).
[30] D. Spaargaren and C. C. Jonker, Nucl. Phys. **A161**, 354 (1971).
[31] I. J. Thompson, Comput. Phys. Rep. **7**, 167 (1988).
[32] B. A. Watson, P. P Singh, and R. E. Segel, Phys. Rev. **182**, 977 (1969).
[33] J.-P. Jeukenne, A. Lejeune, and C. Mahaux, Phys. Rev. C **10**, 1391 (1974).
[34] J.-P. Jeukenne, A. Lejeune, and C. Mahaux, Phys. Rev. C **15**, 10 (1977).
[35] J.-P. Jeukenne, A. Lejeune, and C. Mahaux, Phys. Rev. C **16**, 80 (1977).
[36] A. Lejeune, Phys. Rev. C **21**, 1107 (1980).
[37] J. S. Petler, M. S. Islam, R. W Finlay, and F. S. Dietrich, Phys. Rev. C **32**, 673 (1985).
[38] J. S. Nodvik, C. B. Duke, and M. A. Melkanoff, Phys. Rev. **125**, 975 (1962).
[39] M. El-Azab Farid and G. R. Satchler, Nucl. Phys. **A438**, 525 (1985).
[40] S. Raman, C. H. Malarkey, W. T. Milner, C. W. Nestor, Jr., and P. H. Stelson, At. Data Nucl. Data Tables **36**, 1 (1987).
[41] R. H. Spear, At. Data Nucl. Data Tables **42**, 55 (1989).
[42] G. R. Satchler and W. G. Love, Phys. Rep. **55**, 183 (1979).
[43] N. Vinh Mau, Nucl. Phys. **A592**, 33 (1995).
[44] P. G. Hansen, A. S. Jensen, and B. Jonson, Annu. Rev. Nucl. Part. Sci. **45**, 591 (1995).
[45] J. S. Winfield, S. Fortier, W. N. Catford, S. Pita, N. A. Orr, J. Van de Wiele, Y. Blumenfeld, R. Chapman, S. P.G. Chappell, N. M. Clarke, N. Curtis, M. Freer, S. Galès, H. Langevin-Joliot, H. Laurent, I. Lhenry, J. M. Maison, P. Roussel-Chomaz, M. Shawcross, K. Spohr, T. Suomijärvi, and A. de Vismes, Nucl. Phys. **A632**, 19 (1998).
[46] D. L. Auton, Nucl. Phys. **A157**, 305 (1970).
[47] B. Zwieglinski, W. Benenson, R. G.H. Robertson, and W. R. Coker, Nucl. Phys. **A315**, 124 (1979).
[48] F. Ajzenberg-Selove, Nucl. Phys. **A506**, 1 (1990).
[49] H. Sagawa, Phys. Lett. B **286**, 7 (1992).
[50] H. Iwasaki, T. Motobayashi, H. Akiyoshi, Y. Ando, N. Fukuda, H. Fujiwara, Zs. Fülöp, K. I. Hahn, Y. Higurashi, M. Hirai, I. Hisanaga, N. Iwasa, T. Kijima, T. Minemura, T. Nakamura, M. Notani, S. Ozawa, H. Sakurai, S. Shimoura, S. Takeuchi, T. Teranishi, Y. Yanagisawa, and M. Ishihara, Phys. Lett. B **481**, 7 (2000).
[51] F. M. Nunes, I. J. Thompson, and R. C. Johnson, Nucl. Phys. **A596**, 171 (1996).
[52] R. Bhattacharya and K. Krishan, Phys. Rev. C **56**, 212 (1997).
[53] N. K. Timofeyuk and R. C. Johnson, Phys. Rev. C **59**, 1545 (1999).
[54] X. Liu, M. A. Famiano, W. G. Lynch, M. B. Tang, and J. A. Tostevin, nucl-ex/0402012.
[55] K. Ogata, M. Yahiro, Y. Iseri, and M. Kamimura, Phys. Rev. C **67**, 011602 (2003).